The Journal of Neuroscience, April 1991, 11(4): 918–927

Cloning and Expression of an *Aplysia* K^+ Channel and Comparison with Native *Aplysia* K^+ Currents

Paul J. Pfaffinger, Yasuo Furukawa, Biao Zhao, Deborah Dugan, and Eric R. Kandel

Howard Hughes Medical Institute, Center for Neurobiology and Behavior, Department of Physiology and Biophysics, Columbia University, College of Physicians and Surgeons, New York, New York 10032

We describe here the cloning of the *Aplysia* K^+ channel AK01a. AK01a codes for a protein of 515 amino acids, shows considerable homology to other cloned potassium channels, and can be classified as a member of the *Shaker* K^+ channel family. Expression of the AK01a channel in *Xenopus* oocytes produces a rapidly inactivating outward potassium current (I_{AK01a}) resembling the A-type currents of *Drosophila Shaker*. Gating for this current is shifted to potentials considerably more positive than the traditional A-currents of *Aplysia*; we have, however, identified a novel transient potassium current (I_{Adepol}) in a subset of *Aplysia* neurons that has similar gating and pharmacological properties to I_{AK01a}.

Potassium channel currents are major determinants of a cell's excitability and of its pattern of firing action potentials. Consequently, regulation of these channels is important for the cell's behavior. This is most evident in the nervous system, where there are many different K^+ channels, and a variety of cellular responses can be produced by modulating one or another channel. In nerve cells, various K^+ channels can be activated or suppressed over periods ranging from milliseconds to days, and these channels can participate in aspects of synaptic plasticity including forms of short- and long-term memory (Pfaffinger and Siegelbaum, 1990). To understand how different K^+ channels are assembled, expressed in nerve cells, and modulated by second messengers, we have begun to analyze K^+ channels of the *Aplysia* nervous system at the molecular level.

The initial cloning of the *Shaker* K^+ channel in *Drosophila* (Baumann et al., 1987; Kamb et al., 1987, 1988; Papazian et al., 1987; Tempel et al., 1987; Pongs et al., 1988; Schwarz et al., 1988) has allowed the subsequent cloning of other K^+ channel genes in several species based on homology (Baumann et al., 1988; Tempel et al., 1988; Butler et al., 1989; McKinnon, 1989; Stuhmer et al., 1989; Yokoyama et al., 1989; Wei et al., 1990). Most of the cloned K^+ channels are closely related to the *Drosophila Shaker* gene and probably can be considered members of the same gene family. Within this family, amino acid sequence identity can be very high (>60%) even across species. Despite this strong sequence homology, there are some surprising differences in channel properties. For example, *Shaker* from *Drosophila* encodes A-type channels that inactivate rapidly, whereas some *Shaker* genes in mammalian systems encode delayed-rectifier channels that inactivate slowly or not at all (Iverson et al., 1988; Stuhmer et al., 1988, 1989; Timpe et al., 1988; Christie et al., 1989). Moreover, other gene families have also been found that encode different K^+ channels such as *shab, shal,* and *shaw.* This raises the question of how these various cloned K^+ channels correspond to the variety of K^+ channels that exist in the nerve cells from which they were cloned.

So far, studies of the kinetic and pharmacological properties of the cloned channel proteins have been restricted to *Xenopus* oocytes or to other convenient, but still arbitrary, expression systems. Only very limited research has tried to compare these cloned channels to K^+ channels in the neurons in which these genes are normally expressed (Baker and Salkoff, 1990). As a result, it is not yet clear how closely the properties of these expressed channels reflect the properties of channels found in the native neurons. To overcome this limitation, we have begun a molecular analysis of various K^+ channels in the nervous system of the marine invertebrate *Aplysia californica.* This nervous system contains many large identifiable neurons that form well-studied behavioral networks where K^+ channel modulation by various second messengers has been shown to play an important role (Siegelbaum et al., 1982; Walsh and Byrne, 1985). We are trying to use these advantages to examine the molecular nature of the K^+ channels used by individual identified cells. Toward that end, we here describe the cloning of an *Aplysia* K^+ channel and its expression in *Xenopus* oocytes. We also show that the current expressed in oocytes is similar to a novel type of transient K^+ current present in a subset of *Aplysia* neurons.

Materials and Methods

PCR homology screening. We performed homology screening using the polymerase chain reaction (PCR) and TAQ polymerase (Perkin Elmer-Cetus), with oligonucleotide pools as primers (Pfaffinger and Zhao, 1989). The oligonucleotide pools were designed to allow amplification of the DNA sequence found between 2 amino acid sequences that are conserved in both the *Drosophila* and mouse *Shaker* proteins. Location of conserved amino acids on mouse *Shaker* protein are sense, amino acids (AA) 308–314; antisense, AA 361–366; Tempel et al., 1988). Oligonucleotides were synthesized on either the Applied Biosystems Inc. 381A or 380A synthesizers and were purified by acrylamide/urea gel or by use of an OPC cartridge (Applied Biosystems Inc.). Amplification conditions used were 3 min at 50°C, 4 min at 72°C, and 2 min at 95°C on a Perkin Elmer-Cetus Thermocycler. Standard reaction conditions for PCR were used (Saiki et al., 1988). Amplification products were visualized either by ethidium bromide staining or by autoradiography. DNA

Received July 26, 1990; revised Nov. 16, 1990; accepted Nov. 19, 1990.

This work was supported by the Howard Hughes Medical Institute and by an NIMH graduate research assistantship to B.Z. We thank Dr. Michael Knapp for his assistance with molecular biology methodologies, Harriet Ayers and Andrew Krawetz for typing the manuscript, Kathrin Hilten and Sarah Mack for preparation of the figures, and Drs. Tai Kubo and Stephen Siegelbaum for helpful discussions and assistance in preparing the manuscript.

Correspondence should be addressed to Paul Pfaffinger, Ph.D., Division of Neuroscience, Baylor College of Medicine, 1 Baylor Plaza, Houston, TX 77030.

was prepared for cloning and sequencing by reamplification using oligonucleotides with unique 5'-end restriction sites. The DNA was then cut and ligated into pBSM 13- or pKSM13- (Stratagene) and cloned into *E. Coli* B72 cells or XL-1 Blue (Stratagene). Eight colonies were picked and sequenced by the Sanger method using Sequenase [US Biologicals; AK01a, nucleotides (N) 1003–1178]. All 8 clones were identical in sequence except at degenerate positions on the PCR oligonucleotide pools. A large-scale DNA prep of this sequence was prepared from clone 2-2, 1 of the 8 clones picked.

Two additional segments of the channel's sequence were amplified by PCR. The first segment, clone 11-1 (AK01a, N 482–1143), was isolated by amplification between a specific antisense oligonucleotide to clone 2-2 sequence and a sense oligonucleotide pool to conserved K^+ channel sequence. The second clone, clone 61-1 (AK01a, N 1099–1580), was isolated by amplification between a specific sense oligonucleotide to clone 2-2 sequence and a poly-dT oligonucleotide containing 5' restriction sites. This oligonucleotide did not amplify from a polyA tail as expected, but clone 61-1 does provide confirmatory sequence for AK01a through the termination codon.

Library construction and screening. We constructed a randomly primed cDNA library from 5 μg of *Aplysia* nervous system polyA$^+$ RNA. Double-stranded cDNA was synthesized with the BRL (Bethesda Research Laboratories) cDNA synthesis kit using 500 ng of random hexamer primer (Pharmacia) instead of the oligo-dT primer. The cDNA was tailed with dGTP and cloned into the dCTP-tailed Pst 1 site of Bluescript pKSM13- (Stratagene) by annealing of the homopolymer tails (Eschenfeldt et al., 1987). We generated a primary library containing 7×10^6 independent clones by electroporation transformation into *E. Coli* B72 cells (Dower et al., 1988).

For the initial screening, 1.5×10^6 independent clones were plated and screened using replica nylon filters (Micron Separations Inc.). The remaining library was quick-frozen in EtOH/dry ice and stored in liquid nitrogen. The filters were screened with both a randomly primed probe (Pharmacia) from the PCR clone 11-1 and an end-labeled oligonucleotide from the 5' end of clone 11-1 (AK01a, N 565–597; Ausubel et al., 1989). Moderately low-stringency conditions were used in an attempt to identify other related K^+ channel cDNAs [prehybridization and hybridization solutions: 30% formamide, 5 × SSPE, 5 × Denhardt's, 100 μg/ml single-stranded salmon sperm DNA, 0.2% sodium dodecyl sulfate (SDS), 42°C; wash: 2 × SSPE, 0.2% SDS, 50°C]. Isolated positive colonies were restriction mapped, and the full-length clone AK01a was constructed by ligating 2 of the clones (12-1, 17-1) together at their common Esp 1 site (AK01a, N 573). AK01a was sequenced on both strands by the Sanger method using the Sequenase system (US Biologicals), and, where possible, the sequence was confirmed by comparison to the PCR clones 2-2, 61-1, and 11-1.

Southern blot. For Southern blots, each lane contained 10 μg of *Aplysia* genomic DNA digested with various restriction enzymes that did not cut clone 2-2. The DNA was run out on a 0.75% agarose gel, nicked, and transferred to a nylon filter under alkaline conditions. Hybridization was to the insert of clone 2-2 random primer labeled with ^{32}P-dCTP. Prehybridization and hybridization were carried out at 42°C under standard high-stringency conditions (50% formamide, 5 × SSPE, 5 × Denhardt's, 100 μg/ml single-stranded salmon sperm DNA, 0.1% SDS). After overnight hybridization, the blot was washed 4 times at 65°C in 2 × SSPE with 0.2% SDS.

Northern blot. Total RNA was prepared by the LiCl/urea method (Auffray and Rougeon, 1980). RNA was run on a 1% agarose/formaldehyde gel, blotted, and UV cross-linked to nylon filter paper (Biotrace RP, Gelman Sciences; Ausubel et al., 1989). The blot was probed with a ^{32}P-RNA antisense probe synthesized from linearized clone 11-1. Synthesis, labeling, hybridization, and washing conditions were those recommended by Stratagene (Protocol, Cat. No. 200340).

Nuclease protection assay. Total RNA for each tissue was prepared from 30 *Aplysia* by the guanidinium thiocyanate method of Chomczynski and Sacchi (1987). PolyA$^+$ RNA was isolated by column chromatography using oligo-dT cellulose push columns (Stratagene) and was quantified by UV spectrophotometry and actin probe hybridization. Probes used for nuclease protection were 57 bp oligonucleotides in both sense and antisense orientations, with 47 base pairs (bp) that matched the channel sequence (sense and antisense to AK01a, N 1034–1080). The remaining 10 bp on the 3' end did not match to allow differentiation between digested and nondigested probe. The oligonucleotides were kinase end-labeled with ^{32}P-γ-ATP. The nuclease protection assay was performed according to Ausubel et al. (1989). Under the conditions used in the assay, protected probe ran as 2–3 bands approximately 10 bp below undigested probe.

Oocyte injection and recording. Oocytes from *Xenopus laevis* were isolated and prepared for recording according to the method of Dascal et al. (1984). Oocytes were maintained in supplemented ND-96 solution: 96 mM NaCl, 2 mM KCl, 1.8 mM $CaCl_2$, 1 mM $MgCl_2$, 5 mM HEPES (pH, 7.6), supplemented with 2.5 mM sodium pyruvate, 0.5 mM theophylline, and 100 U/ml penicillin/streptomycin, at 18°C (solution changed daily). Oocytes were allowed to recover for 24 hr following isolation, then were injected with *in vitro* transcribed, capped cRNA (Stratagene) from clone AK01a. Approximately 50 nl of cRNA at a concentration of 1 μg/μl was injected into each oocyte. Injected oocytes were maintained in supplemented ND-96 solution for 2–4 d before recording.

For electrical recording, oocytes were placed on a nylon mesh in the recording chamber (0.7 ml). The chamber was continuously perfused with ND-96 (0.4–0.8 ml/min). All drugs were applied by changing the perfusion solution to ND-96 supplemented with the drug. For measurement of reversal potentials, the NaCl in ND-96 was exchanged with KCl in an equimolar fashion.

Oocyte currents were recorded with a 2-microelectrode voltage clamp using a virtual-ground circuit (Dagan 8500, Dagan Corp., Minneapolis, MN). Both recording and current passing electrodes were Ag–AgCl wires in glass pipettes filled with a mixture of 3 M potassium acetate and 0.1 M potassium chloride. The pipette tips were broken back to a resistance of 1–3 Ω. To reduce capacitive coupling, electrodes were wrapped to within 5 mm of the tip with aluminum foil. The voltage-recording electrode's shield was driven; the current electrode's shield was connected to ground. In addition, a grounded shield was placed between the 2 electrodes. The virtual ground was a Ag–AgCl electrode connected to the bath with a 3 M KCl–agar bridge. Stimulation, recording, and data analyses were performed using the BASIC-FASTLAB system run on an AT-compatible computer (Indec Systems, Inc., Sunnyvale, CA).

Aplysia electrophysiology. Aplysia californica (40–50 gm) were anesthetized by intraabdominal injection of isotonic $MgCl_2$, and the abdominal ganglion was dissected out. After treatment of the ganglion for 90 min with 1% protease (Sigma, type IX), the connective sheath was removed by microdissection. Most recordings were made from acutely isolated ganglia. Recordings were in Na^+- and Ca^{2+}-free artificial sea water (Na^+/Ca^{2+}-free ASW: 460 mM Tris, 10 mM KCl, 65 mM $MgCl_2$, 10mM HEPES, pH 7.6) to block Na^+ and Ca^{2+} currents. Potassium channel drugs were prepared in Na^+/Ca^{2+}-free ASW at the concentration used and applied by bath perfusion. The voltage-clamp and recording setup was identical to the system used to record from *Xenopus* oocytes.

Results

Cloning of an Aplysia *K^+ channel*

Homology screening for an *Aplysia* potassium channel was performed using the polymerase chain reaction (PCR). cDNA synthesized from *Aplysia* nervous system RNA was amplified for 35 cycles using oligonucleotides based on sequences conserved between mouse and *Drosophila* K^+ channel clones (Tempel et al., 1988). A single DNA fragment of 176 bp was amplified, cloned (clone 2-2), and sequenced. The deduced amino acid sequence of clone 2-2 [AK01a, AA 342–393] is 85% identical to other *Shaker* sequences, clearly demonstrating that the amplified DNA is part of a K^+ channel.

Two additional segments of this channel's sequence were subsequently isolated using PCR with different sets of oligonucleotides: clone 11-1 (AK01a, N 482–1143) and clone 61-1 (AK01a, N 1099–1580).

To confirm that the amplified DNA is from an *Aplysia* sequence, and not from some contaminating DNA in the amplification reaction, we probed a Southern blot of *Aplysia* genomic DNA with a random primer labeled probe from clone 2-2. One to 2 bands were visible in DNA cut with different enzymes, confirming the cDNA we have cloned is part of an *Aplysia* gene. We therefore proceeded to clone the entire coding region for this gene.

To clone the entire coding region for this K^+ channel, we

```
                                                5'-....AAACCCTGTATTGTTAGTTCTCACGACTAAACTGTGAATGTAATAACGCGT   -191

CTGGTAAAGTCGCGTGTGTGACGTCAAAATAATCGATTTCATCCGGGGAACAAACGTATTATTTTTGTCCGCCATATTTGTAGATTTGTTATGAT              -96

CAAAGTGGTTAAAAAACCGCACGCTGGAATGGCAGGCGCGTGTTGCTTGGTCACTGAGACTTTGTATGTAAGGGTGGACTAATGCAGGCAGTAAA              -1

Met Glu Val Ala Met Ala Gly Ile Glu Gly Asn Gly Gly Pro Ala Gly Tyr Arg Asp Ser Tyr His Ser Ser    24
ATG GAG GTT GCT ATG GCT GGG ATC GAG GGT AAC GGC GGC CCG GCT GGC TAC CGG GAC AGC TAC CAT TCA TCC    72

Gln Arg Pro Leu Leu Arg Ser Ser Asn Leu Pro Asn Ser Arg Ser Phe Pro Lys Leu Ser Glu Glu Asp Asn    48
CAA CGG CCA CTT TTA CGC TCT TCT AAT CTT CCA AAT TCC AGG TCT TTT CCC AAG CTC TCA GAG GAA GAC AAT    144

Ala Asn Glu Asn Gly Met Gly Val Pro Gly Ser Asp Tyr Asp Cys Ser Cys Glu Arg Val Val Ile Asn Val    72
GCC AAT GAG AAT GGG ATG GGC GTG CCC GGG AGC GAC TAT GAC TGC AGC TGT GAG CGC GTG GTG ATC AAC GTG    216

Ser Gly Leu Arg Phe Glu Thr Gln Leu Lys Thr Leu Asn Gln Phe Pro Asp Thr Leu Leu Gly Asn Pro Gln    96
AGC GGT CTC CGG TTC GAG ACG CAG CTG AAA ACC CTC AAC CAG TTC CCC GAT ACG TTG CTT GGC AAT CCT CAA    288

Lys Arg Asn Arg Tyr Tyr Asp Pro Leu Arg Asn Glu Tyr Phe Phe Asp Arg Asn Arg Pro Ser Phe Asp Ala    120
AAG CGA AAC CGC TAT TAC GAC CCA CTT CGC AAC GAG TAT TTC TTT GAC AGG AAT CGA CCC AGT TTT GAC GCA    360

Ile Leu Tyr Phe Tyr Gln Ser Gly Gly Arg Leu Arg Arg Pro Val Asn Val Pro Leu Asp Val Phe Ser Glu    144
ATC TTG TAT TTC TAC CAG AGC GGC GGC CGG TTA CGG AGG CCC GTG AAC GTT CCC TTG GAT GTG TTC TCA GAG    432

Glu Ile Lys Phe Tyr Glu Leu Gly Glu Asn Ala Phe Glu Arg Tyr Arg Glu Asp Glu Gly Phe Ile Lys Glu    168
GAG ATC AAG TTT TAT GAG CTG GGA GAG AAT GCC TTT GAG AGG TAC AGA GAA GAT GAG GGC TTC ATC AAA GAG    504

Glu Glu Lys Pro Leu Pro Gln Asn Glu Phe Gln Arg Arg Val Trp Leu Leu Phe Glu Tyr Pro Glu Ser Ser    192
GAA GAG AAG CCT TTG CCA CAG AAT GAG TTT CAG AGG AGA GTG TGG CTG TTG TTT GAG TAC CCT GAG AGC TCA    576

                                                    S1
Ala Ala Ala Arg Leu Cys Ala Ile Phe Ser Val Val Ile Ile Leu Leu Ser Ile Val Ile Phe Cys Leu Glu    216
GCG GCT GCC AGG CTC TGC GCC ATC TTC TCT GTA GTC ATT ATC CTT TTG TCC ATT GTT ATA TTC TGT TTG GAG    648

Thr Leu Pro Gln Phe Lys His Tyr Arg Val Val Asn Ser Thr Ala Asn Asp Ser Lys Glu Ser Ile Glu Glu    240
ACT TTA CCA CAA TTC AAG CAT TAC AGG GTG GTC AAC TCG ACG GCC AAT GAT TCG AAA GAG TCC ATT GAG GAG    720

                                                                S2
Asp Asp Ile Pro Lys Phe Asn Glu Pro Phe Phe Ile Ile Glu Thr Cys Cys Ile Ile Trp Phe Thr Phe Glu    264
GAT GAT ATT CCA AAG TTC AAT GAG CCC TTC TTC ATC ATT GAG ACC TGT TGC ATC ATC TGG TTC ACA TTT GAG    792

Leu Leu Val Arg Phe Ala Ser Cys Pro Glu Lys Leu Gly Phe Phe Lys Asn Ile Met Asn Cys Ile Asp Ile    288
CTT TTG GTG AGG TTT GCT TCG TGC CCA GAG AAG CTC GGC TTC TTC AAG AAC ATC ATG AAC TGC ATT GAC ATT    864

                    S3
Val Ala Ile Ile Pro Tyr Phe Ile Thr Leu Gly Thr Val Val Ala Asp Gln Ser Lys Ser Asn Asn Gln Ala    312
GTC GCT ATC ATT CCA TAC TTC ATC ACT CTG GGC ACG GTG GTG GCC GAC CAG AGC AAG AGC AAT AAT CAA GCC    936

                                                S4
Met Ser Leu Ala Ile Leu Arg Val Ile Arg Leu Val Arg Val Phe Arg Ile Phe Lys Leu Ser Arg His Ser    336
ATG TCT CTG GCC ATC CTC AGG GTC ATC CGA TTG GTC AGG GTC TTC AGG ATA TTC AAA CTT TCC AGA CAC TCG    1008

Lys Gly Leu Gln Ile Leu Gly Gln Thr Leu Lys Ala Ser Met Arg Glu Leu Gly Leu Leu Ile Phe Phe Leu    360
AAA GGC CTT CAG ATC CTA GGC CAG ACC CTC AAA GCC AGT ATG CGA GAA CTG GGC CTG CTC ATA TTC TTC CTC    1080

          S5
Phe Ile Gly Val Ile Leu Phe Ser Ser Ala Val Tyr Phe Ala Glu Ala Asp Ala Asp Gln Thr His Phe Lys    384
TTC ATA GGT GTT ATT TTG TTT TCC AGT GCT GTC TAC TTT GCC GAG GCT GAC GCC GAC CAG ACC CAC TTT AAA    1152

Ser Ile Pro Asp Ala Phe Trp Trp Ala Val Val Thr Met Thr Thr Val Gly Tyr Gly Asp Met Arg Pro Ile    408
AGT ATT CCC GAT GCA TTC TGG TGG GCC GTG GTC ACC ATG ACG ACG GTG GGC TAC GGA GAC ATG CGG CCG ATC    1224

                                                        S6
Gly Val Trp Gly Lys Leu Val Gly Ser Leu Cys Ala Ile Ala Gly Val Leu Thr Ile Ala Leu Pro Val Pro    432
GGG GTG TGG GGC AAG CTG GTT GGC TCT CTG TGC GCC ATC GCT GGC GTG CTC ACG ATC GCG CTT CCT GTC CCT    1296

Val Ile Val Ser Asn Phe Asn Tyr Phe Tyr His Arg Glu Gly Glu Ser Thr Asp Lys Gly Gln Tyr Lys His    456
GTC ATT GTG TCT AAT TTC AAC TAT TTC TAC CAT CGA GAA GGG GAG AGC ACT GAC AAG GGA CAG TAC AAG CAC    1368
                                  *
Val Gln Ser Cys Pro Asn Tyr Pro Glu Lys Lys Asp Ser Leu Asp Ser Glu Cys Gly Ser Asp Ile Met Glu    480
GTG CAG TCC TGC CCC AAC TAC CCC GAG AAA AAA GAT TCT TTG GAT TCT GAG TGC GGC TCG GAT ATC ATG GAG    1440

Met Glu Glu Gly Asn His Ser Thr Pro Leu Thr Glu Lys Val Lys Glu Asn His Ala Ile Lys Ala Asn Asn    504
ATG GAG GAG GGC AAC CAC AGC ACT CCG CTG ACG GAG AAG GTG AAA GAG AAC CAT GCA ATC AAG GCC AAT AAC    1512

Pro Gly Ser Asp Tyr Gly Leu Glu Thr Asp Val ***                                                    515
CCC GGC AGT GAC TAC GGG CTG GAG ACT GAC GTA TGA CACAGTGCCTCGCTACAACTTCCAGCATTGAACGCTCCTTTGCTATA    1595

GGGAGACCATTGCGGCATGACATGAACTTGCGCTCATCCGCGCAGACTTTCTGTCGTTCCTCGCAAGATTCGAGTGAAGAGGATCTCAGAATTTT    1690

TTT....-3'
```

Figure 1. Sequence of clone AK01a and primary amino acid sequence of deduced protein. Sequences of 6 putative transmembrane segments (*S1–S6*) are indicated by *boxes*. Two proposed sites of N-linked glycosylation are *underlined*. Putative cAMP-dependent protein kinase phosphorylation site indicated by an *asterisk*.

constructed and screened a primary, randomly primed, plasmid cDNA library using the insert of clone 11-1 as a probe. Nine positive clones were isolated from 1.5×10^6 colonies. These clones covered the entire coding region of this *Aplysia* K^+ channel. The full-length clone AK01a was constructed from 2 clones isolated from the randomly primed cDNA library (clones 12-1, 17-1), by ligating the 5′ end of clone 12-1 to the 3′ end of clone 17-1 at their common Esp 1 site (AK01a, N 573).

Sequence analysis

The full-length *Aplysia* clone AK01a codes for a protein of 515 amino acids and a calculated molecular weight of 58,604 Da (Fig. 1). The protein has a calculated acidic pI due to an excess of negative over positive charge. Like other K^+ channels, there is no leader signal peptide sequence; therefore, the amino terminus is presumed to be intracellular. An examination of the hydropathy plot for AK01a (Fig. 2*A*) reveals the structural homology of this protein to other K^+ channels. Like other K^+ channels, there are 6 putative transmembrane domains (S1–S6) each longer than 18 AA, together with a short hydrophobic segment (AA 389–400) that is presumably too short to cross the lipid bilayer. This topology would also assign the carboxy terminus to be intracellular. Like other K^+ channels, the fourth transmembrane segment (S4) is an amphipathic helix where every third amino acid residue is positively charged and is presumably the primary voltage sensor for the channel.

Figure 2*B* shows a schematic diagram of the membrane topology of AK01a and the location of several functional sites, along with amino acid residues that are conserved between AK01a and *Shaker* type K^+ channels from several species. Consistent with this topology are proposed N-linked glycosylation sites (Asn: 228, 232) on the extracellular segment between S1 and S2 and a conserved phosphorylation site for the cAMP-dependent protein kinase (Ser: 469) on the C-terminal intracellular segment. Although the region of highest homology to other K^+ channels is located in the central core of the protein (AA 60–470), the amino acid residues at both the carboxy and amino termini have also been conserved. The 5 amino terminal amino acid residues (MEVAM) are identical to those of RCK4 (Stuhmer et al., 1989), and the carboxy terminal tripeptide (TDV) is conserved for all *Shaker* K^+ channels.

Northern blot

To examine both the quantity and the size of the mRNA for AK01a, we performed a Northern blot analysis on nervous system RNA. Fifteen micrograms of nervous system total RNA were run on an agarose/formaldehyde gel, blotted, and probed with an antisense RNA probe synthesized from clone 11-1. A single band was seen at a very high molecular weight, >12 kilobases (kb; Fig. 3*A*). Extrapolation on a semilogarithmic plot of the RNA ladder migration gives a band size of approximately 15 kb. This band was not seen with sense RNA probes and was present in polyA$^+$ RNA, confirming the large size of the mRNA for the *Aplysia Shaker* homolog AK01a.

Distribution of AK01a in Aplysia

The tissue distribution of AK01a expression in *Aplysia* was examined using an S1 nuclease protection assay (Fig. 3*B*). PolyA$^+$ RNA was prepared from several different tissues. One microgram of polyA$^+$ RNA from each tissue was allowed to anneal overnight to either a sense or an antisense oligonucleotide, and then free oligonucleotide was digested with S1 nuclease. AK01a mRNA was detected by its protection of the antisense probe,

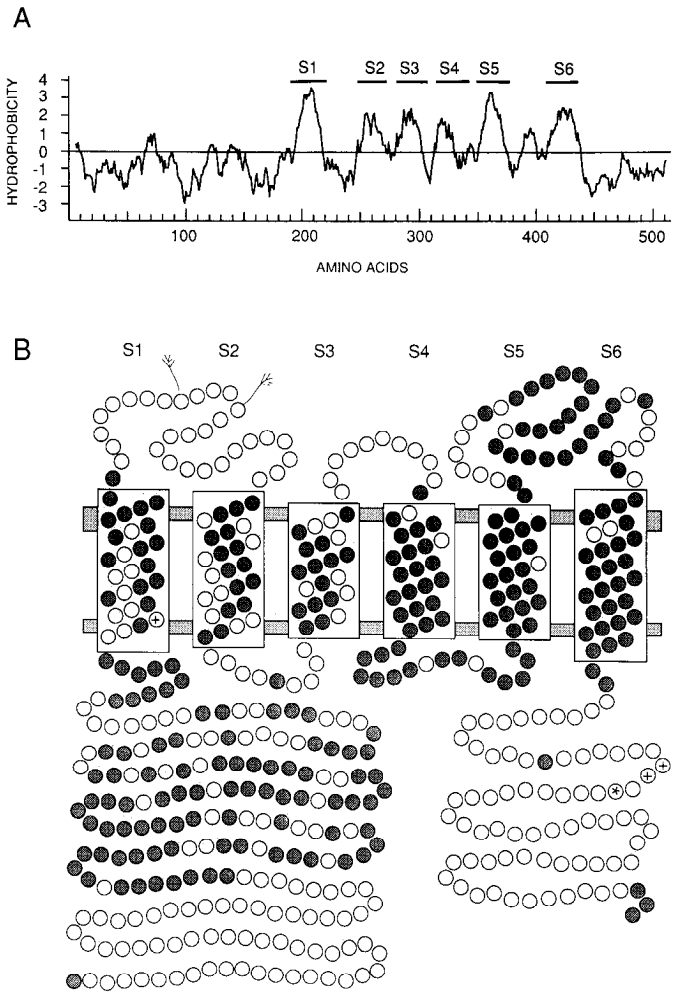

Figure 2. Homology of AK01a to other K^+ channels. *A*, Kyte–Doolittle hydropathy plot of AK01a shows the 6 large peaks (*S1–S6*) of hydrophobicity characteristic of K^+ channels. *B*, Schematic folding of AK01a in membrane shown along with location of amino acids conserved between AK01a and *Shaker*-type K^+ channels from several species. Transmembrane segments are the same as those indicated in *A*. *Solid circles* indicate amino acids conserved between AK01a and *Shaker*-type K^+ channels cloned from other species, pluses indicate conserved positive charges (Baumann et al., 1988; Kamb et al., 1988; Pongs et al., 1988; Schwarz et al., 1988; Tempel et al., 1988; McKinnon, 1989; Stuhmer et al., 1989). A pair of glycosylation sites between S1 and S2 are shown (Asn: 228, 232). A conserved cAMP-dependent protein kinase site on a C-terminal intracellular segment is indicated (*asterisk*; Ser: 469).

but not the sense probe, from digestion with S1 nuclease. mRNA for AK01a was detected in CNS, heart, gill muscle, and buccal muscle, but not in ovotestis. The relative abundance was CNS $\gg$ heart = gill muscle > buccal muscle.

Expression in Xenopus *oocytes*

We next examined the properties of the channel encoded by clone AK01a using the *Xenopus* oocyte expression system. Enzymatically desheathed oocytes (stages V–VI) were injected with 50 nl of capped RNA (1 μg/μl) transcribed *in vitro* from clone AK01a. Two to four days following injection of RNA, a new transient outward current (I_{AK01a}) was recorded from the oocytes (Fig. 4*A*). From a holding potential of −80 mV, the current activates in response to depolarizations more positive than −20 mV, reaching a peak amplitude of 1–3 μA at 40 mV, then

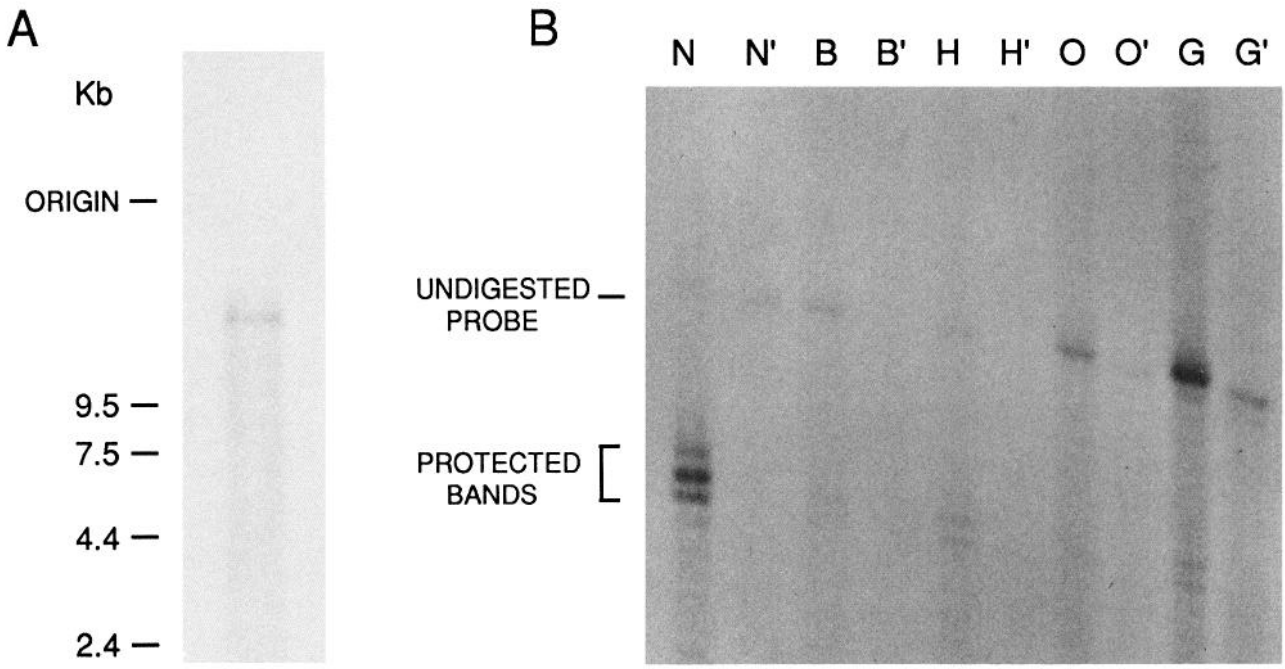

Figure 3. **AK01a messenger RNA size and distribution.** *A,* Northern blot on 15 μg of total nervous system RNA probed with antisense ^{32}P-RNA probe synthesized from clone 11-1. After exposure for 3 d at −70°C with enhancer screens, a single band of ≈15 kb was seen. *B,* Nuclease protection assays using sense and antisense oligonucleotides to AK01a sequence. *N* and *N′,* nervous system; *B* and *B′,* buccal muscle; *H* and *H′,* heart muscle; *O* and *O′,* ovotestis; *G* and *G′,* gill muscle. Antisense probe, *N, B, H, O, G*; sense control probe, *N′, B′, H′, O′, G′.* The protected probe runs as 2–3 bands approximately 10 bp below the undigested probe. The autoradiogram was overexposed to show weak bands.

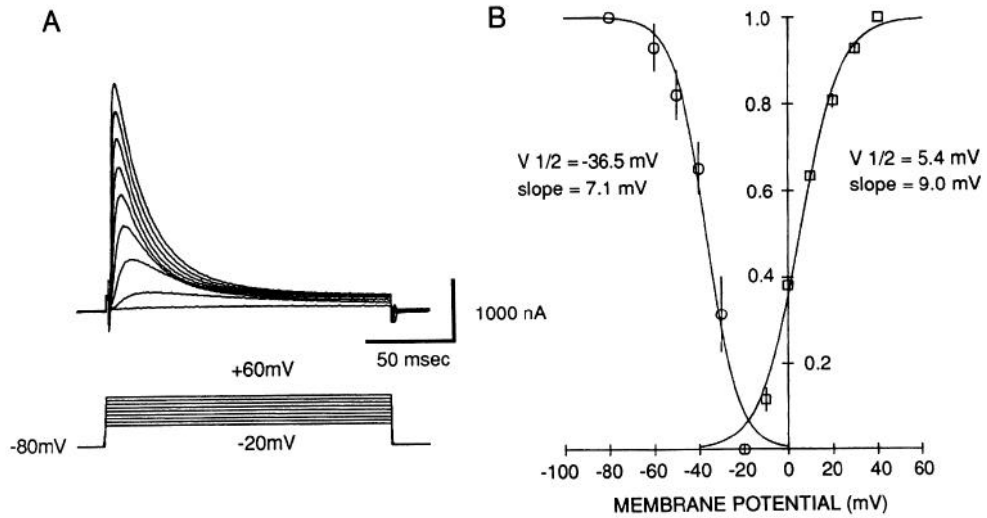

Figure 4. Expression of AK01a in *Xenopus* oocytes. *A,* Membrane currents expressed in *Xenopus* oocyte 2 d after injection of *in vitro*-transcribed AK01a RNA. Membrane potential was stepped from −20 mV to 60 mV in 10-mV increments from the holding potential of −80 mV. *B,* Activation (□; $n = 4$) and inactivation (○; $n = 3$) properties of AK01a. Inactivation curve (h_∞) was constructed by varying the holding potential and measuring the peak current in response to a constant test depolarization to 20 mV. Values are normalized to peak current measured from a holding potential of −80 mV. The *smooth lines* are Boltzmann fits to the data using the formula $I_{norm} = 1/(1 + \exp((E - V_{1/2}/K))$; where E = holding potential, $V_{1/2}$ = potential where half-inactivated, and K = slope factor. The activation curve was constructed by measuring the peak conductance (G_{peak}) of the 4-AP-sensitive current (see Fig. 6*B*) to minimize the influence of native oocyte currents. Conductance was calculated using the equation $G_{peak} = I_{peak}(E - E_{rev})$, where E is the test potential and E_{rev} is the reversal potential of the expressed current (−83 mV). Activation data were fit with a Boltzmann distribution. *Error bars* represent SD.

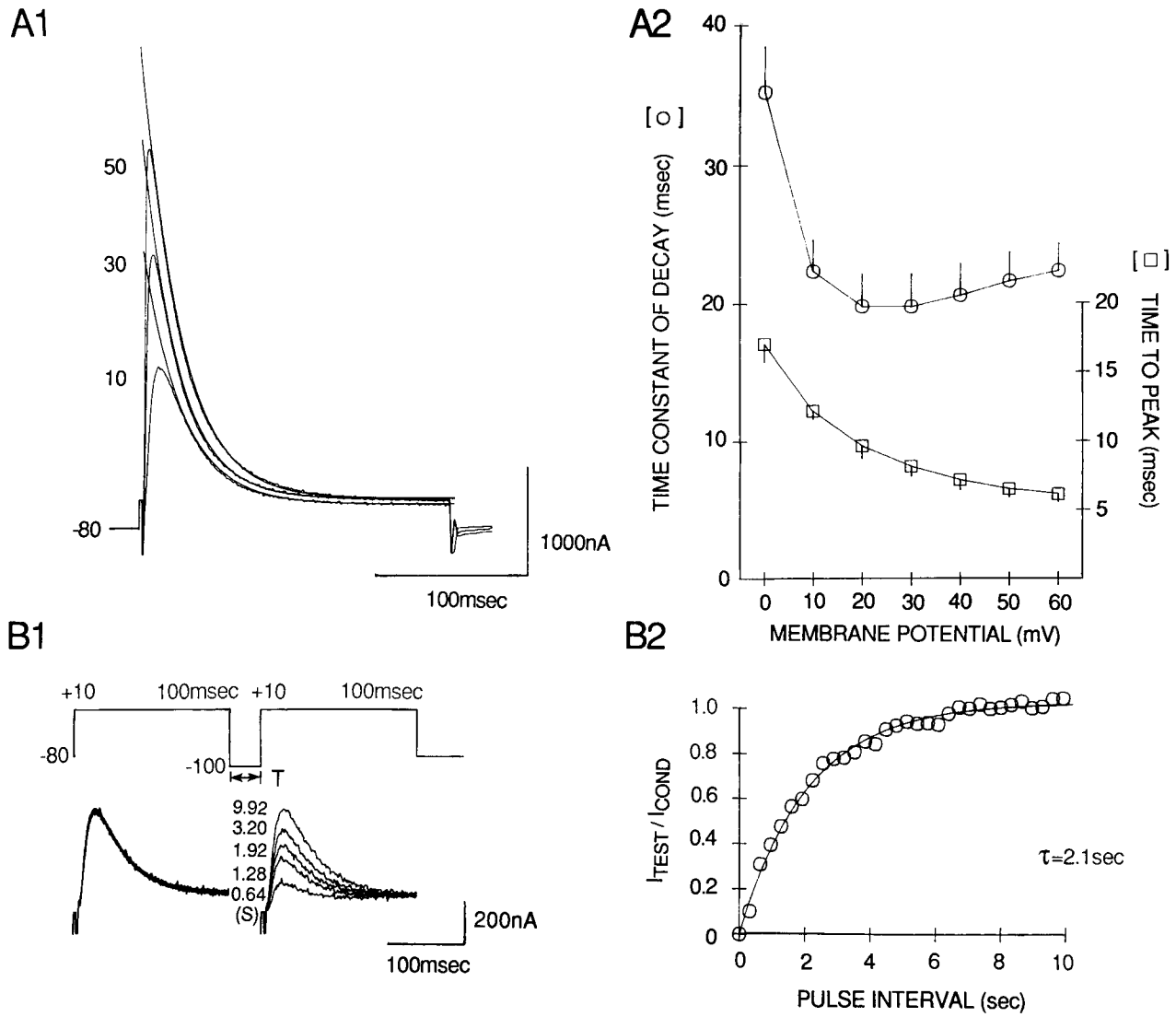

Figure 5. Gating of I_{AK01a}. *A*, Kinetic properties of I_{AK01a} activation and inactivation. *A1*, Inactivation of I_{AK01a} is well fit by a single exponential. *A2*, Time to peak (□; $n = 3$) and inactivation time constant (○; $n = 3$) measured for different test potentials. *Error bars* represent SD. *B*, Recovery from inactivation measured using a 2-pulse protocol. *B1*, Recovery of current in second pulse following varying lengths of time at −100 mV. Seconds at −100 mV are indicated next to each current trace. *B2*, Plot of peak current in second pulse versus length of time at −100 mV. Currents were normalized by peak current of first pulse. The *line* is an exponential fit to the data with a time constant of 2.1 sec.

inactivates completely within 120 msec. The current was unaffected by perfusion of the bath with Ca-free solutions.

Voltage dependence of I_{AK01a}

Figure 4*B* shows the voltage dependence of steady-state inactivation (h_∞) and peak conductance for the expressed channels. The steady-state inactivation curve could be approximated by a Boltzmann distribution having a midpoint of −36.5 mV and a slope of 7.1 mV. The peak conductance curve has a half-activation at +5.4 mV, a slope of 9.0 mV, and little overlap with the steady-state inactivation curve.

Kinetics of I_{AK01a}

The rates of activation and inactivation of the macroscopic currents showed some voltage dependence (Fig. 5*A*). For activation, the time to peak decreased steadily from 17 msec at 0 mV to 6 msec at 40 mV. Inactivation was well fit with a single exponential (Fig. 5*A1*). The time constant for inactivation decreased from 35 msec at 0 mV to 20 msec at 20 mV but was relatively constant at potentials more positive than 20 mV. At potentials more negative than 0 mV, the rate of inactivation proceeded much more slowly.

We also examined the rate of recovery from inactivation using a 2-pulse protocol (Fig. 5*B*). The amplitude of I_{AK01a} was first recorded by stepping to 10 mV from a holding potential of −80 mV. Then, the voltage was held for variable lengths of time at −100 mV before a second pulse to 10 mV was applied. The ratio of (peak current during 2d pulse):(peak current during 1st pulse) was plotted versus the duration of the hyperpolarization. The time course of the recovery could be fit with a single exponential having a time constant of 2.3 ± 0.5 sec ($n = 5$) at −100 mV.

Ionic selectivity of I_{AK01a}

To examine the ionic basis of I_{AK01a}, we measured the reversal potential of tail currents at the peak activation of I_{AK01a}. The

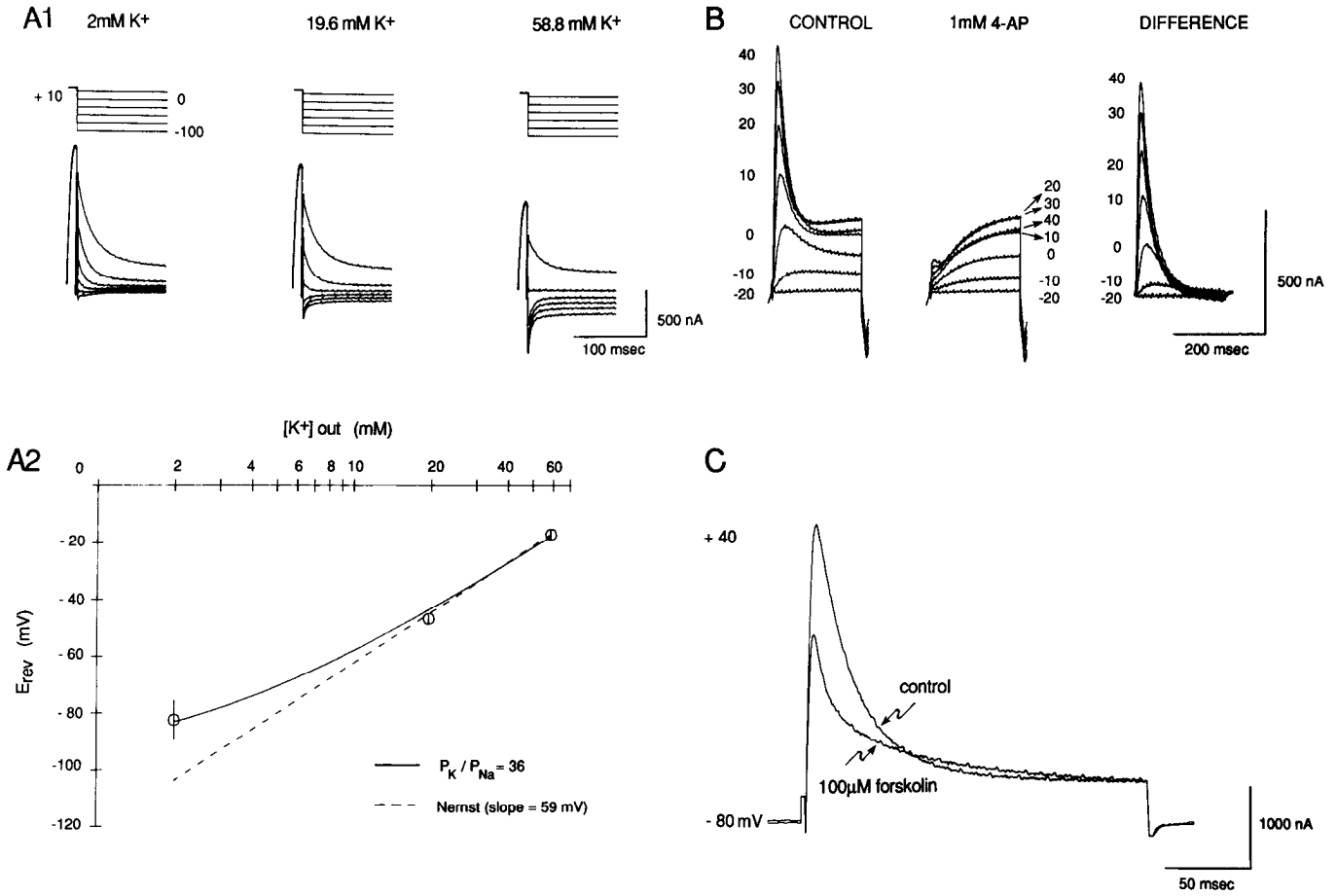

Figure 6. Pharmacological properties of I_{AK01a}. *A,* Reversal potential of I_{AK01a} at different external K^+ concentrations. *A1,* Reversal of I_{AK01a} tail currents measured at 20-mV increments from 0 to −100 mV. Following equimolar substitution of K^+ for Na^+ in the bath solution, reversal potential shifted to more positive potentials. *A2,* Plot of E_{rev} versus external K^+ concentration. The *broken line* shows the K^+ Nernst potential. The *solid line* shows the fit of data to the Goldman–Hodgkin–Katz equation with a P_K:P_{Na} ratio of 36:1. *Error bars* represent SD. *B,* Block of I_{AK01a} with 1 mM 4-AP. Remaining currents in 1 mM 4-AP are Ca^+-activated Cl^- currents. Difference currents show that I_{AK01a} inactivates completely during the depolarization. *C,* Sensitivity of I_{AK01a} to 100 μM forskolin. A single 200-msec depolarization to +40 mV is shown in the presence and absence of 100 μM forskolin. Forskolin depresses the peak and changes the shape of inactivation from a single to a double exponential decay. Note that, despite the decrease in peak current, the current trace for 100 μM forskolin crosses over the control trace later in the pulse as a result of a change in the shape of inactivation.

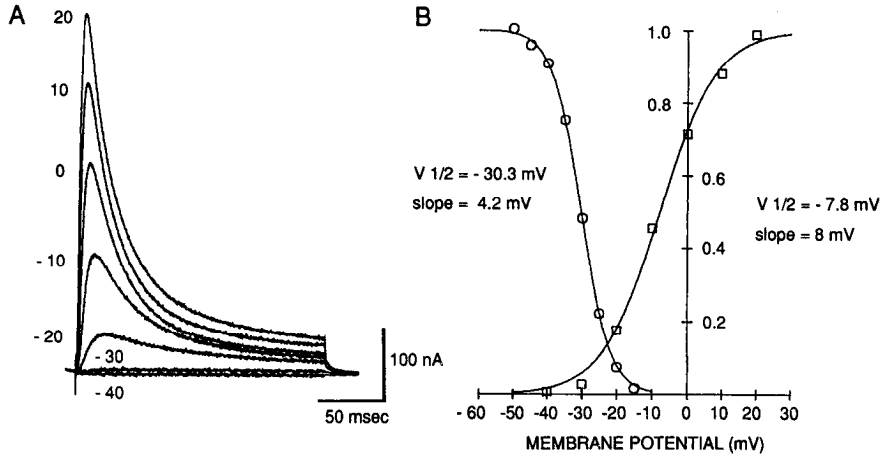

Figure 7. I_{Adepol} recorded in R15 neuron from *Aplysia* abdominal ganglion. *A,* I_{AD} current traces recorded as the difference current between current traces recorded with 1-sec prepulses to −20 or −50 mV. The current inactivated by a prepulse to −20 mV but not −50 mV is largely composed of I_{Adepol}. Traces were recorded in Na^+/Ca^{2+}-free ASW with 50 mM TEA to reduce the size of delayed-rectifier currents. *B,* Activation and inactivation properties of $I_{A\text{-}depol}$. Inactivation (○) of I_{Adepol} was measured with a test pulse to 0 mV following 2-sec prepulses at potentials from −50 to −15 mV. Activation (□) of I_{Adepol} was measured as peak conductance during the test depolarization assuming $E_{rev} = E_K = -89$ mV. Data for activation and inactivation were fit with the Boltzmann distribution.

Table 1. Comparison of native *Aplysia* K^+ currents to I_{AK01a}

	I_{Afast}	I_{Aslow}	I_{Adepol}	I_{AK01a}
Activation				
Midpoint (mV)	−23.6	−27.8	−7.8	+5.4
Boltzmann slope	8.2	8.4	8.0	9.0
Time to peak (msec)[a]	3.4	7.1	8.3	9.1
Inactivation				
Midpoint (mV)	−69.7	−73.2	−29.9	−20.9
Boltzmann slope	5.7	4.7	4.1	3.3
Decay τ (msec)[b]	4.8	54.1	26.3	22.3
Recovery from Inactivation (msec)	60.7[c]	135.8[c]	360[d] (19,000)[d]	2,300[c] (18,000)[d]
Blockers				
TEA[e]	−	−	−	−
4-AP (1 mM)[f]	+	+	+++	+++
MCDP (1 μM)	−	ND	ND	−
Forskolin (100 μM)				
Peak depression	25%	35%	40–60%	40%
Inactivation[g]	−	2 τ	2 τ	2 τ

ND, not determined; −, no effect; +, weak effect; +++, strong effect.

[a] Value measured near peak of activation: I_{Afast} = −5 mV; I_{Aslow} = −5 mV; I_{Adepol} = 20 mV; I_{AK01a} = 40 mV.

[b] Value measured near peak of activation: I_{Afast} = −10 mV; I_{Aslow} = −15 mV; I_{Adepol} = 40 mV; I_{AK01a} = 60 mV.

[c] Slightly different pulse protocol used to record recovery of I_{Afast} and I_{Aslow}. Potential where recovery is measured: I_{Afast} = −90 mV; I_{Aslow} = −90 mV; I_{AK01a} = −100 mV. Recovery for these currents can be fit with a single exponential.

[d] Isolation of I_{Adepol} requires measurement of recovery at −50 mV to inactivate I_{Afast}. Recovery of I_{Adepol} has 2 exponentials. The faster recovery rate constitutes about 75% of the total recovery. Slower recovery rate is given in parentheses. For comparison, the recovery time constant of I_{AK01a} at −50 mV is given in parentheses.

[e] TEA tested at 50 mM in neurons and 10 mM in oocytes.

[f] 4-AP completely blocks I_{Adepol} and I_{AK01a} at 1 mM. I_{Afast} and I_{Aslow} are half-blocked at 5 mM 4-AP.

[g] Effect of forskolin on shape of inactivation indicated. I_{Afast} inactivation was unaffected. Forskolin modifies inactivation of I_{Adepol}, I_{Aslow}, and I_{AK01a} to double exponential decay:

I_{Aslow}: at −15 mV, τ inactivation was 77.1 msec (control), 10.4 msec, and 386 msec (forskolin).

I_{AK01a}: at 10 mV, τ inactivation was 20.9 msec (control), 15.4 msec, and 111.2 msec (forskolin).

I_{Adepol}: at 10 mV, τ inactivation was 21.4 msec (control), 9.88 msec, and 94.6 msec (forskolin).

change in reversal potential was measured as external Na^+ was progressively replaced with K^+. Figure 6*A* shows E_{rev} plotted against the log of K_o. The reversal potential follows the Nernst potential for K^+ at higher concentrations as expected for a K^+-permeable channel, but at low K^+ concentrations, the reversal potential is more positive than the K^+ Nernst potential, suggesting that the channel is slightly permeable to Na, with a P_K:P_{Na} ratio of 36:1.

Pharmacology of I_{AK01a}

We next examined the effect of various K^+ channel drugs on I_{AK01a}. I_{AK01a} was not blocked by bath application of 10 mM tetraethylammonium (TEA), 200 nM charybdotoxin, or 1 μM mast cell degranulating peptide (MCDP); however, the current was sensitive to the K^+ channel blocker 4-aminopyridine (4-AP). I_{AK01a} was completely blocked by 1 mM 4-AP (Fig. 6*B*). The current remaining after 4-AP application is the native oocyte Ca-dependent Cl current (Barish, 1983). A plot of the 4-AP sensitive current, calculated as the difference current following application of 4-AP to an oocyte expressing I_{AK01a}, confirms that I_{AK01a} completely inactivates during the depolarization.

We also examined the effect of forskolin on I_{AK01a} (Fig. 6*C*). Although originally thought to act only by activation of adenylate cyclase, forskolin has recently been shown in some cases to block K^+ channels independent of increases in intracellular cAMP (Coombs and Thompson, 1987). Application of 100 μM forskolin to oocytes expressing I_{AK01a} decreased the peak current and changed the kinetics of inactivation from a single exponential to a double exponential. The peak current was decreased by 40% in 100 μM forskolin, independent of membrane potential. Although the peak current was depressed and the initial decay of I_{AK01a} was faster following forskolin application, the presence of a second slower time constant caused the forskolin-modified current trace to cross over the control current and thus be larger than control I_{AK01a} later in the pulse.

Although the channel has a putative cAMP-dependent protein kinase phosphorylation site, the effect of forskolin was not caused by activation of adenylate cyclase, because application of the cell-permeable, nonhydrolyzable derivative 1 mM 8(4cpt)-cAMP had no effect on I_{AK01a}. In addition, the forskolin derivative 1,9-dideoxyforskolin, which is inactive on adenylate cyclase, had qualitatively similar effects to forskolin on I_{AK01a}, though the maximal effect was smaller than that of forskolin. Because 1,9-dideoxyforskolin is relatively insoluble in the recording solution used here, this weaker effect may not necessarily reflect a lower potency, but rather a lower applied concentration.

Comparison of I_{AK01a} *with native transient* K^+ *currents of* Aplysia *neurons*

Aplysia neurons contain at least 2 types of traditional A-currents, I_{Afast} and I_{Aslow}, distinguished by their different rates of inactivation (Y. Furukawa, E. R. Kandel, and P. Pfaffinger, unpub-

lished observations). The gating of I_{AK01a} expressed in *Xenopus* oocytes occurs at potentials considerably more positive than usual for these traditional A-currents of *Aplysia* neurons (Byrne, 1980; Furukawa, Kandel, and Pfaffinger, unpublished observations). We therefore tested whether these neurons also contained another transient potassium current active at more positive potentials. Figure 7 shows one such current (I_{Adepol}; an *A*-current gating at *depol*arized potentials) isolated from the R15 neuron of the abdominal ganglion of *Aplysia*. Because this neuron also contains a traditional A-current (I_{Afast}) and a large delayed-rectifier current, several steps were needed to isolate I_{Adepol}: First, the bath solution contained 50 mM TEA, which blocks most delayed-rectifier currents. Second, a 1-sec prepulse to −50 mV was applied before the test pulse to selectively inactivate I_{Afast}. Because complete recovery of I_{Adepol} from inactivation is slow, the cell is held for 20 sec at −80 mV between pulses.

The current traces in Figure 7*A* are difference currents from R15 showing currents that are inactivated by a 1-sec prepulse to −20 mV but not by a 1-sec prepulse to −50 mV. These currents are largely composed of I_{Adepol}. As can be seen in Figure 7*B*, the activation and inactivation of I_{Adepol} occurs at quite depolarized potentials.

Table 1 compares the properties of I_{AK01a} to I_{Adepol} and to the two *Aplysia* A-currents that gate at the traditional potentials for *Aplysia* A-currents. We have examined each current in detail in a specific identified cell in which the current is particularly well expressed. I_{Afast}, a rapidly inactivating A-current, was studied in LUQ cells. I_{Aslow}, a slower inactivating A-current, was studied in RUQ cells. Also, I_{Adepol}, the transient K^+ current gating at more depolarized potentials, was studied in R15. A more complete characterization of these native *Aplysia* K^+ currents is being made by Furukawa, Kandel, and Pfaffinger (unpublished observations).

Discussion

We have cloned and expressed an *Aplysia* K^+ channel, AK01a. The mRNA for AK01a is exceptionally long, >12 kb. Long mRNAs have been seen for other channels, but none with quite so much excess. It is unclear what role, if any, this excess RNA plays in the control of AK01a expression. AK01a expression is not limited to the nervous system; nuclease protection assays also identify the RNA in other excitable tissues, buccal muscle, heart muscle, and gill smooth muscle, but not in the nonexcitable immature ovotestis. Further experiments will be needed to show conclusively that AK01a expression is limited to excitable tissues.

The protein encoded by the *Aplysia* clone AK01a shows high homology, ≈70% identity, to *Shaker* potassium channel clones from other species. This confirms the importance of these conserved residues to K^+ channel function, particularly when one considers the great evolutionary distance between mammals, *Aplysia*, and *Drosophila* and the fact that the salt-water environment of the *Aplysia* would seem to exert unique evolutionary pressures on ion channels. Electrophysiologically, we find that the AK01a potassium channel is more similar to the *Drosophila Shaker* channels than to the mammalian *Shaker* channels, because it inactivates rather rapidly during a depolarization. In addition, we have recently isolated a clone identical to AK01a except at the 5′ end (not shown), suggesting the AK01a gene may be alternatively spliced like *Drosophila Shaker*. This conclusion remains tentative pending complete sequencing, expression, and characterization of this putative alternative splice.

A comparison between I_{AK01a} and three transient K^+ currents in *Aplysia* neurons reveals a gradient of shared properties between these currents. I_{AK01a} is most different from I_{Afast}. Although both are blocked by 4-AP (I_{Afast} is less sensitive to 4-AP) and not by TEA, few other properties are similar. It seems likely that I_{Afast} channels are composed of protein subunits from a different gene than AK01a, as has been suggested for the fast A-current of *Drosophila* and *Shaker* A-currents (Solc et al., 1987).

I_{AK01a} is more similar to I_{Aslow}. Again, both are blocked by 4-AP and not by TEA. In addition, the inactivation time constant is not voltage dependent at potentials more positive than the midpoint of the activation curve (data not shown for I_{Aslow}). Also, like I_{AK01a}, forskolin application causes a reduction in the I_{Aslow} peak current and changes the gating kinetics of inactivation from a single to a double exponential. For both the native I_{Aslow} and the oocyte-expressed I_{AK01a} channels, the forskolin effect is not due to changes in cAMP: application of 8(4cpt)-cAMP has no effect, while 1,9-dideoxyforskolin has qualitatively similar effects to forskolin without affecting adenylate cyclase. Because oocytes have an elevated resting level of cAMP (Dascal, 1987), this does not rule out some effect of cAMP-dependent protein kinase on the putative phosphorylation site of AK01a.

However, despite these similarities, the oocyte-expressed current I_{AK01a} can easily be distinguished from I_{Aslow} on the basis of several important electrophysiological criteria: Activation and inactivation of I_{Aslow} occur at considerably more negative potentials than do those of I_{AK01a} (approximately 40 mV more negative). I_{AK01a} recovers from inactivation much more slowly than I_{Aslow}. I_{Aslow} is less sensitive to 4-AP than is I_{AK01a}. Finally, the decay rate of I_{Aslow} is 2 times slower than that of I_{AK01a}. It is unclear, therefore, whether I_{Aslow} is encoded by a different gene, is a heteromultimeric channel including AK01a subunits, or represents current through modified or alternatively spliced AK01a channels.

The K^+ current in *Aplysia* that most closely resembles I_{AK01a} is I_{Adepol}. Unlike traditional A-currents, the activation and inactivation properties of I_{Adepol} are shifted to potentials considerably more depolarized than the resting potential and almost as positive as I_{AK01a}. Also, the pharmacological properties of I_{AK01a} are most similar to I_{Adepol}: both currents are blocked by 1 mm 4-AP and not blocked by TEA. The time constant for inactivation and the response to forskolin are also very similar between I_{AK01a} and I_{Adepol}. A careful comparison of activation and inactivation properties does reveal some differences between I_{AK01a} and I_{Adepol}. Several possible explanations for these differences are (1) incomplete isolation of I_{Adepol}, so that other currents contribute to activation and inactivation curves; (2) allelic variations in the wild *Aplysia* population causes subtle differences in the properties of currents made from the AK01a gene; (3) splice variants of AK01a, or other proteins, contribute to forming the I_{Adepol} channel; (4) posttranslational processing differences, membrane properties of *Aplysia* neurons, or different ionic environments make the same channel protein function differently in *Xenopus* oocytes than in *Aplysia* neurons; or (5) I_{Adepol} is encoded by a different gene.

In future experiments, we plan to examine these possibilities by (1) using single-channel recording to compare I_{Adepol} and I_{AK01a} more accurately; (2) characterizing a possible alternative splice of the AK01 gene and specifically checking for additional alternative splicing, using nuclease protection assays; (3) express-

ing AK01a by DNA or cRNA microinjection into *Aplysia* neurons to examine the influence of the expression environment; and (4) studying the properties of other K^+ channel genes cloned from *Aplysia.*

In other experiments, we are also exploring where the AK01a channel is normally expressed in the nervous system, what role this channel plays in a neuron, and how its expression and distribution are controlled.

References

Auffray C, Rougeon F (1980) Purification of mouse immunoglobulin heavy-chain messenger RNAs from total myeloma tumor RNA. Eur J Biochem 107:303–314.

Ausubel FM, Brent R, Kingston RE, Moore DD, Seidman JG, Smith JA, Struhl K (1989) Current protocols in molecular biology. New York: Wiley.

Baker K, Salkoff L (1990) The *Drosophila Shaker* gene codes for a distinctive K^+ current in a subset of neurons. Neuron 2:129–140.

Barish ME (1983) A transient calcium-dependent chloride current in the immature *Xenopus* oocyte. J Physiol (Lond) 342:309–325.

Baumann A, Kraj-Jentgens I, Muller R, Muller-Holtkamp F, Seidel R, Kecskemethy N, Casal J, Ferrus A, Pongs O (1987) Molecular organization of the maternal effect region of the *Shaker* complex of *Drosophila*: characterization of an I_A channel transcript with homology to vertebrate Na channel. EMBO J 6:3419–3429.

Baumann A, Grupe A, Ackermann A, Pongs O (1988) Structure of the voltage-dependent potassium channel is highly conserved from *Drosophila* to vertebrate central nervous systems. EMBO J 7:2457–2463.

Butler A, Wei A, Baker K, Salkoff L (1989) A family of putative potassium channel genes in *Drosophila.* Science 243:943–947.

Byrne JH (1980) Analysis of ionic conductance mechanisms in motor cells mediating inking behavior in *Aplysia californica.* J Neurophysiol 43:630–650.

Chomczynski P, Sacchi N (1987) Single step method of RNA isolation by acid guanidinium thiocyanate-pheno-chloroform extraction. Anal Biochem 162:156–159.

Christie MJ, Adelman JP, Douglass J, North RA (1989) Expression of a cloned rat brain potassium channel in *Xenopus* oocytes. Science 244:221–224.

Coombs J, Thompson SJ (1987) Forskolin's effect on transient K current in *Nudibranch* neurons is not reproduced by cAMP. J Neurosci 7:443–452.

Dascal N (1987) The use of *Xenopus* oocytes for the study of ion channels. CRC Crit Rev Biochem 22:317–387.

Dascal N, Landau EM, Lass Y (1984) *Xenopus* oocyte resting potential, muscarinic responses and the role of calcium and guanosine 3′-5′-cyclic monophosphate. J Physiol (Lond) 352:551–574.

Dower WJ, Miller SF, Ragsdale CW (1988) High efficiency transformation of *E. coli* by high voltage electroporation. Nucleic Acids Res 16:6127–6145.

Eschenfeldt WH, Puskas RS, Berger SL (1987) Homopolymeric tailing. Meth Enzymol 152:337–342.

Iverson LE, Tanouye MA, Lester HA, Davidson N, Rudy B (1988) A-type potassium channels expressed from *Shaker* locus cDNA. Proc Natl Acad Sci USA 85:5723–5727.

Kamb A, Iverson LE, Tanouye MA (1987) Molecular characterization of *Shaker,* a *Drosophila* gene that encodes a potassium channel. Cell 50:405–413.

Kamb A, Tseng-Crank J, Tanouye MA (1988) Multiple products of the *Drosophila Shaker* gene may contribute to potassium channel diversity. Neuron 1:421–430.

McKinnon D (1989) Isolation of a cDNA clone coding for a putative second potassium channel indicates the existence of a gene family. J Biol Chem 264:8230–8236.

Papazian DM, Schwarz TL, Tempel BL, Jan YN, Jan LY (1987) Cloning of genomic and complementary DNA from *Shaker,* a putative potassium channel gene from *Drosophila.* Science 237:749–753.

Pfaffinger PJ, Siegelbaum SA (1990) K^+ channel modulation by G proteins and second messengers. In: Potassium channels: structure, classification, function and therapeutic potential (Cook NS, ed), pp 117–153. Chicester: Norwood.

Pfaffinger PJ, Zhao B (1989) PCR based homology screening and cloning of a voltage gated potassium channel from *Aplysia* central nervous system. J Cell Biochem [Suppl] 13E:301.

Pongs O, Kecskemethy N, Muller R, Krah-Jentgens I, Baumann A, Kiltz HH, Canal I, Llamarares S, Ferrus A (1988) *Shaker* encodes a family of putative potassium channel proteins in the nervous system of *Drosophila.* EMBO J 7:1087–1096.

Saiki RK, Gelfand DH, Stoffel S, Scharf SJ, Higuchi R, Horn GT, Mulis KB, Erlich HA (1988) Primer-directed enzymatic amplification of DNA with a thermostable DNA polymerase. Science 239:487–491.

Schwarz LT, Tempel BL, Papazian DM, Jan YN, Jan LY (1988) Multiple potassium-channel components are produced by alternative splicing at the *Shaker* locus in *Drosophila.* Nature 331:137–142.

Siegelbaum SA, Camardo J, Kandel ER (1982) Serotonin and cyclic AMP close single K^+ channels in *Aplysia* sensory neurones. Nature 299:413–417.

Solc CK, Zagotta WN, Aldrich RW (1987) Single-channel and genetic analyses reveal two distinct A-type potassium channels in *Drosophila.* Science 236:1094–1098.

Stuhmer W, Stocker M, Sakmann B, Seeburg P, Baumann A, Grupe A, Pongs O (1988) Potassium channels expressed from rat brain cDNA have delayed rectifier properties. FEBS Letts 242:199–206.

Stuhmer W, Ruppersberg JP, Schroter KH, Sakmann B, Stacker M, Giese KP, Perschke A, Baumann A, Pongs O (1989) Molecular basis of functional diversity of voltage-gated potassium channels in mammalian brain. EMBO J 8:3235–3244.

Tempel BL, Papazian DM, Schwarz TL, Jan YN, Jan LY (1987) Sequence of a probable potassium channel component encoded at the *Shaker* locus in *Drosophila.* J Neurosci 7:1307–1317.

Tempel BL, Jan YN, Jan LY (1988) Cloning of a probable potassium channel from mouse brain. Nature 332:837–839.

Timpe LC, Schwarz TL, Tempel BL, Papazian DM, Jan YN, Jan LY (1988) Expression of functional potassium channels from *Shaker* cDNA in *Xenopus* oocytes. Nature 331:143–145.

Walsh JP, Byrne JH (1985) Analysis of decreased conductance serotonergic response in *Aplysia* ink motor neurons. J Neurophysiol 53: 590–601.

Wei A, Corarrublas M, Butler A, Baker K, Pak M, Salkoff L (1990) K^+ current diversity is produced by an extended gene family conserved in *Drosophila* and mouse. Science 248:599–603.

Yokoyama S, Imoto K, Kawamura T, Higashida H, Naoyuki I, Miyata T, Numa S (1989) Potassium channels from NG108-15 neuroblastoma-glioma hybrid cells. FEBS Letts 259:37–42.